applied sciences

MDPI

Article

# A New Smart Grid Hybrid DC–DC Converter with Improved Voltage Gain and Synchronized Multiple Outputs

**Khaled A. Mahafzah [1], Mohammad A. Obeidat [2], Ayman Mansour [2], Eleonora Riva Sanseverino [3] and Gaetano Zizzo [3,*]**

[1] Department of Electrical Engineering, Faculty of Engineering, Al-Ahliyya Amman University, Amman 19328, Jordan; k.mahafzah@ammanu.edu.jo
[2] Electrical Power and Mechatronics Engineering Department, Tafila Technical University, Tafila 66110, Jordan; maobaidat76@ttu.edu.jo (M.A.O.); mansour@ttu.edu.jo (A.M.)
[3] Department of Engineering, University of Palermo, 90128 Palermo, Italy; eleonora.rivasanseverino@unipa.it
* Correspondence: gaetano.zizzo@unipa.it

**Abstract:** This paper introduces a new hybrid DC–DC converter with enhanced voltage gain and synchronized multiple output capabilities, specifically tailored for smart grid applications. The proposed converter is based on the integration of non-isolated Zeta and Mahafzah converters, comprising a single controlled switch, two diodes, three inductors, and two coupling capacitors. The primary objective of this novel hybrid converter is to improve voltage gain as compared to conventional Zeta and Mahafzah topologies. By achieving higher voltage gain at lower duty cycles, the converter effectively reduces voltage stress on semiconductor switches and output diodes, thereby enhancing overall performance and reliability. A comprehensive examination of the hybrid converter's operating principle is presented, along with detailed calculations of duty cycle and switching losses. The paper also explores the converter's application in smart grids, specifically in the context of renewable energy systems and electric vehicles. Two distinct scenarios are analyzed to evaluate the converter's efficacy. Firstly, the converter is assessed as a DC–DC converter for renewable energy systems, highlighting its relevance in sustainable energy applications. Secondly, the converter is evaluated as an electric vehicle adapter, showcasing its potential in the transportation sector. To validate the converter's performance, extensive simulations are carried out using MATLAB/SIMULINK with parameters set at 25 kW, 200 V, and 130 A. The simulation results demonstrate the converter's ability to efficiently supply multiple loads with opposing energy flows, making it a promising technology for optimized grid management and energy distribution. Moreover, the paper investigates the total harmonic distortion (THD) of the grid current, focusing on its impact in smart grid environments. Notably, the new hybrid converter topology achieves a THD of 21.11% for the grid current, indicating its ability to effectively mitigate harmonics and improve power quality. Overall, this research introduces a cutting-edge hybrid DC–DC converter that enhances voltage gain and synchronizes multiple outputs, specifically catering to the requirements of smart grid applications. The findings underscore the converter's potential to significantly contribute to the advancement of efficient and resilient power conversion technologies for smart grids, enabling seamless integration of renewable energy systems and electric vehicles into the grid.

**Keywords:** hybrid converter; HVDC grid; Zeta converter; Mahafzah converter; THD; EV charger

check for updates

**Citation:** Mahafzah, K.A.; Obeidat, M.A.; Mansour, A.; Sanseverino, E.R.; Zizzo, G. A New Smart Grid Hybrid DC–DC Converter with Improved Voltage Gain and Synchronized Multiple Outputs. *Appl. Sci.* **2024**, *14*, 2274. https://doi.org/10.3390/app14062274

Academic Editor: Kambiz Vafai

Received: 29 January 2024
Revised: 3 March 2024
Accepted: 6 March 2024
Published: 8 March 2024

**Copyright:** © 2024 by the authors. Licensee MDPI, Basel, Switzerland. This article is an open access article distributed under the terms and conditions of the Creative Commons Attribution (CC BY) license (https://creativecommons.org/licenses/by/4.0/).

## 1. Introduction

Power electronics DC–DC converters find wide-ranging applications in various fields, including hybrid energy systems (that use two or more renewable energy resources), hybrid vehicles (that use energy storage systems and fuel energy), aerospace, satellite technology, and portable electronic devices. Extensive research efforts have been dedicated to improving the reliability, efficiency, modularity, and cost-effectiveness of these converters.

The evolution of DC–DC converter topologies has led to the development of versatile solutions capable of handling multiple applications and output voltage levels. However, as the demands for advanced power conversion systems continue to grow, it becomes evident that no single topology can fully meet all the diverse requirements of cost-effectiveness, reliability, flexibility, efficiency, and modularity.

Hybrid DC–DC converters have emerged as a promising approach to addressing these challenges effectively. Hybrid DC–DC converters combine multiple converter topologies or techniques to achieve specific performance objectives. By integrating the advantages of different converter types, these hybrid solutions can optimize efficiency, voltage regulation, power density, and other desired characteristics. Extensive investigations and analyses of various hybrid converter configurations have been conducted and documented in the literature.

This paper presents a comprehensive overview of different hybrid DC–DC converter topologies, highlighting their advantages and providing literature reviews for each one. The goal is to explore the potential of hybrid converters as versatile solutions for power electronics applications. By identifying the strengths and weaknesses of various hybrid configurations, researchers and practitioners can better design and implement efficient power conversion systems tailored to meet the specific requirements of diverse applications. The insights gained from the literature review will pave the way for the development of innovative and optimized hybrid DC–DC converters capable of addressing the evolving needs of modern power electronics technology.

The buck-boost converter offers several distinct advantages in DC–DC power conversion. One of its benefits is the ability to regulate the output voltage efficiently, ensuring a stable voltage level even when the input voltage fluctuates or is higher or lower than the desired output. Moreover, its bidirectional operation allows for both step-up and step-down voltage conversion, offering versatility for a wide range of applications [1].

In [2], the SEPIC-Cuk converter has the ability to provide noninverting voltage conversion. The output voltage can be either higher or lower than the input voltage. This flexibility is valuable in applications where the input voltage varies or is unstable. The converter also features continuous input and output current, enabling it to handle varying load demands efficiently. Additionally, the SEPIC-Cuk converter's bidirectional operation makes it suitable for battery charging applications, where it can efficiently step up or step down the voltage as needed. The limitation of the SEPIC-Cuk converter is the complexity of the design.

Ref. [3] introduced flyback-forward converter; this hybrid configuration has the ability to provide isolated output, making it suitable for applications where galvanic isolation is necessary to ensure safety and reduce noise interference. The flyback-forward converter also offers a wide input voltage range and good voltage regulation capabilities, accommodating varying input voltages and providing stable output. Moreover, it can efficiently step up or step down the voltage, allowing for versatile voltage conversion. Its complex topology makes the design and control more challenging compared to individual converters, potentially leading to higher development costs.

In [4], the full-bridge LLC (LCC) converter is a popular DC–DC converter topology known for its high efficiency and robust performance. One of its primary advantages is its ability to achieve zero-voltage switching (ZVS) and zero-current switching (ZCS) during the switching transitions, reducing switching losses and increasing overall efficiency. This advantage makes it well-suited for high-power applications, where minimizing power losses is crucial. The full-bridge LLC converter also provides isolation between the input and output, ensuring safety and reducing noise interference in sensitive applications. Additionally, its full-bridge configuration allows bidirectional power flow, making it suitable for applications where power can flow in both directions, such as in renewable energy systems. Its complex topology and control requirements can make the design and implementation more challenging compared to simpler converters, potentially increasing development costs and time.

In [5], a newly developed power electronic converter that combines elements of both the flyback and Cuk converter topologies is introduced. The converter is designed to provide multiple output voltages with synchronization between the outputs. Combining flyback and Cuk topologies in a hybrid configuration, allows for the generation of multiple output voltages while maintaining synchronization between them. The design and control of the synchronized multiple output DC–DC converter improve the performance of the converter, including efficiency, voltage regulation, and transient response. This converter can be applied in various fields, including power supplies, telecommunications, electric vehicles, and renewable energy systems. It offers a compact and efficient solution for generating multiple synchronized output voltages from a single input source.

The flyback-SEPIC Converter also offers galvanic isolation between the input and output, ensuring safety and reducing ground loop issues in sensitive systems. Moreover, it can achieve continuous input and output current, enabling it to handle fluctuating load demands efficiently [6]. Different hybrid DC–DC converter topologies based on different references are presented in Table 1 with their advantages.

**Table 1.** Different hybrid DC–DC converter topologies.

| Literature Review | Hybrid DC–DC Converter | Topologies Combined | Advantages |
|---|---|---|---|
| [1,2,7–10] | Buck-Boost Converter | Buck, Boost | Voltage step-up and step-down capability, flexible voltage conversion, wide input range |
| [2,11–14] | SEPIC-Cuk Converter | SEPIC, Cuk | Wide input voltage range, galvanic isolation, continuous currents, |
| [3,15–18] | Flyback-Forward Converter | Flyback, forward | Bidirectional power flow, multiple isolated outputs |
| [4,19–22] | Full-Bridge LLC Converter | Full-Bridge, LLC | High efficiency, high power density, low EMI |
| [23–27] | Hybrid Multilevel Converter | Various multilevel topologies | High voltage, high power, reduced harmonics, low switching losses |
| [5,28,29] | Flyback-Cuk Converter | Flyback, CuK | High efficiency, high voltage regulation, improved transient response |
| [6,14,30] | Flyback-SEPICConverter | Flyback, SEPIC | High efficiency, High voltage regulation, improved transient response |
| **Main Features Comparison** | | | |
| **Hybrid converter** | **Number of Outputs** | **Voltage Gain** | **THD** |
| [5] | 2 | $\frac{V_o}{V_{in}} = \left\lvert \frac{N_s - N_p}{N_p} \frac{D_M}{1-D_M} \right\rvert$ | 27.69% |
| [6] | 2 | $\frac{V_o}{V_{in}} = \frac{N_2+N_1}{N_1} \frac{D_M}{1-D_M}$ | 27.26% |
| **Proposed converter** | 3 | $\frac{V_{o3}}{V_{in}} = \frac{2D_M}{1-D_M}$ | 21.11% |

A type of DC–DC power converter called a Zeta converter, see Figure 1, can change voltage in both step-up and step-down directions. They were created by combining buck and boost converters, and they have characteristics in common with the cuk converter [31]. Because of their versatility and high efficiency, Zeta converters are utilized in a wide range of applications, including telecommunications, solar energy harvesting, and battery-powered systems. One of the key benefits of the Zeta converter is its ability to maintain consistent input and output currents. These properties have the advantages of lower

electromagnetic interference (EMI), lower input and output current ripple, and improved dependability. Additionally, the Zeta converter may provide input-output isolation upon request, broadening its use.

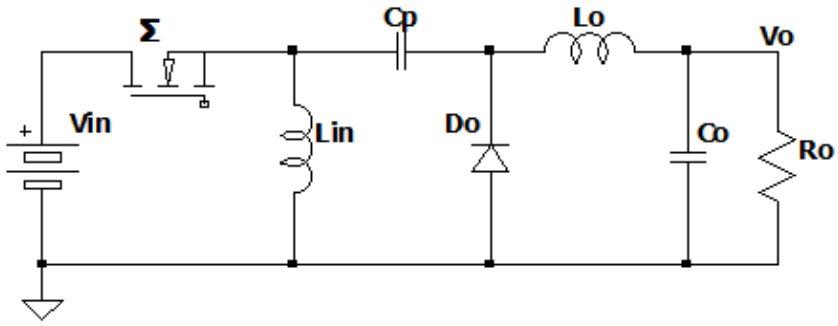


**Figure 1.** Zeta converter.

In contrast to the conventional Cuk converter, the newly introduced Mahafzah converter [32], depicted in Figure 2, exhibits several notable advantages, including increased efficiency, a more compact footprint, and reduced semiconductor device currents. While the essential components of the Cuk converter are retained in the proposed design, they are arranged in a novel configuration without the need for any additional components.

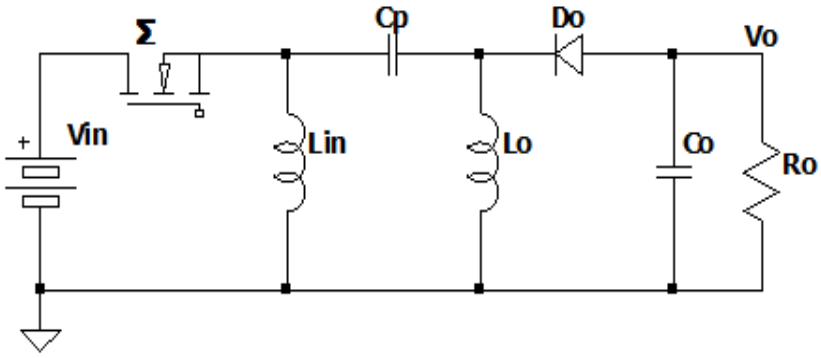


**Figure 2.** Mahafzah converter.

A significant advantage of the suggested Mahafzah converter lies in its use of a coupling capacitor with a substantially lower rated voltage as compared to the Cuk converter. As a result, the coupling capacitor's size is reduced, leading to a smaller printed circuit board (PCB) and lowering manufacturing costs. Moreover, this innovative design choice contributes to decreased semiconductor device currents, enhancing the overall converter efficiency.

For the evaluation of its efficiency, the converter operates in continuous current mode (CCM) with a fixed duty cycle and switching frequency, demonstrating its superior performance characteristics [31]. By showcasing the efficiency gains and practical benefits, the Mahafzah converter offers a promising alternative to traditional Cuk converters, making it an attractive option for various power electronics applications.

This paper proposes a new hybrid converter based on two combined, non-isolated DC–DC converters. The latter being a Zeta converter with a Mahafzah converter [32]. The proposed hybrid converter comprises one controlled switch, two diodes, two coupling capacitors, three inductors, and two low-pass filters. Moreover, the proposed hybrid converter can supply three different loads, including one with inverted polarity. The proposed hybrid converter has an improved voltage gain and, therefore, lower voltage stress across the controlled switch. This voltage stress reduction leads to lower conduction losses and, thus, higher efficiency.

In this paper, we introduce a comprehensive study aimed at defining a novel converter design tailored to meet the evolving demands of smart grids. The rapid evolution of

power systems necessitates adaptable converter solutions capable of seamlessly integrating with emerging technologies and accommodating diverse operational requirements [33]. Our research addresses this imperative by proposing a new converter design specifically engineered to enhance compatibility with modern smart grid infrastructures. This design draws inspiration from a wide array of cutting-edge technologies, including wind, tidal, fuel cell, and photovoltaic generation, as well as various storage solutions, FACT devices, HVDC lines, and power-electronics-interfaced loads [34]. By synthesizing insights from these key components, our study aims to pioneer a converter solution optimized for the dynamic challenges and opportunities presented by the contemporary energy landscape [35].

This paper presents a significant contribution in the realm of power electronics DC–DC converters, focusing on the development of a new hybrid converter that combines the advantages of two non-isolated DC–DC converter topologies: the Zeta converter and the Mahafzah converter. The primary objective of this research is to design a converter that can deliver improved voltage gain and synchronized multiple output voltages, making it particularly suitable for smart grid applications. The contribution of this paper can be summarized as follows:

- Development of a New Hybrid Converter: The paper introduces a novel hybrid DC–DC converter that integrates elements from both the Zeta converter and the Mahafzah converter. By combining these converter topologies, the proposed hybrid converter achieves enhanced voltage gain, contributing to higher efficiency and reduced voltage stress on the controlled switch.
- Improved Efficiency and Performance: Through the integration of the Zeta and Mahafzah converters, the new hybrid converter offers improved performance characteristics, such as better voltage regulation and transient response. The synchronization between multiple output voltages ensures seamless operation and optimal power delivery, making it an attractive solution for various applications.
- Multi-Load Capability: The proposed hybrid converter is designed to supply three different loads, including one with inverted polarity. This flexibility in load handling expands the converter's versatility, making it suitable for a wide range of applications.
- Architecture and Design Analysis: The paper thoroughly discusses the architecture and design of the proposed hybrid converter. It includes detailed parameter selection and loss calculations, providing valuable insights into the converter's operational behavior and efficiency.
- Application Scenarios: The research presents two different applications of the proposed hybrid converter. The first scenario involves its use as a DC–DC converter, while the second explores its application as an AC–DC converter. This demonstrates the converter's adaptability in diverse energy conversion tasks.
- Practical Implementations: The findings of this paper have the potential for practical implementation in various fields, including power supplies, telecommunications, electric vehicles, and renewable energy systems. The compact and efficient nature of the hybrid converter offers a viable solution for generating multiple synchronized output voltages from a single input source.

In summary, this research contributes to the advancement of hybrid DC–DC converters for smart grid applications by proposing a new topology that combines the Zeta and Mahafzah converter principles. The improved voltage gain, synchronized multiple outputs, and flexible load handling make the proposed hybrid converter an appealing option for achieving higher efficiency and enhanced performance in power conversion systems. The practical applications and design insights presented in this paper pave the way for further developments in the field of power electronics.

The rest of the paper can be summarized as follows: Section 2 discusses the hybrid converter architecture and proposes the design of the proposed hybrid converter with the selection of its parameters and its associated loss calculation. Section 3 addresses two different applications of the proposed hybrid converter. The first one is the use of the

proposed converter in a DC–DC conversion. The second one is the use of the proposed hybrid converter in an AC–DC conversion. Section 4 concludes the work.

## 2. The Proposed Converter

This section addresses the new converter architecture, design, modeling, and simulation.

### 2.1. The Proposed Converter Architecture

The proposed converter comprises of two different non-isolated DC–DC converter topologies. The first one is the Zeta converter (Figure 1). The second one is the Mahafzah converter (Figure 2) [32]. Figure 3 shows the proposed converter. From Figure 3, it can be seen that the proposed converter has only one common DC power supply $V_{in}$, one common controlled switch M, and one common input inductance $L_{in}$. Moreover, the proposed converter has three separate output terminals (the voltage across the third output is the sum of $V_{o1}$ + $V_{o2}$). Two coupling capacitors, $C_{p1}$ and $C_{p2}$, and two output inductors, $L_{o1}$ and $L_{o2}$, are used to limit the energy transfer to the output terminals.

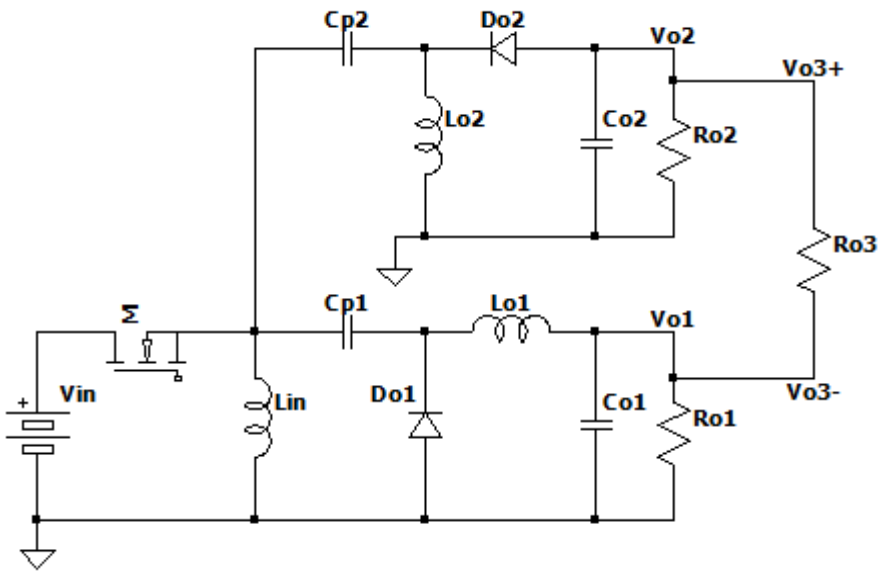


**Figure 3.** The proposed converter with three output voltages.

### 2.2. The Proposed Converter Modeling and Design

The proposed converter has two operating periods during a full switching cycle, $T_s$. The proposed converter is operated in continuous conduction mode (CCM). Therefore, the two sub-periods depend on the switch M status.

- During $T_{on}$ of M, both $D_{o1}$ and $D_{o2}$ are in reverse bias. The inductors' currents' directions are shown in Figure 4.

  The inductors' currents are given by:

$$I_{Lin} = \frac{V_{in}}{L_{in}} t + I_{Lin-min} \tag{1}$$

$$I_{Lo1} = \frac{V_{in-} V_{cp1} - V_{o1}}{L_{o1}} t + I_{Lo1-min} \tag{2}$$

$$I_{Lo2} = \frac{V_{in-} V_{cp2}}{L_{o2}} t + I_{L2-min} \tag{3}$$

where $0 < t < T_{on}$, $I_{Lin\text{-}min}$, $I_{L1min}$ and $I_{L2min}$ are the lower limits of the inductor's currents.

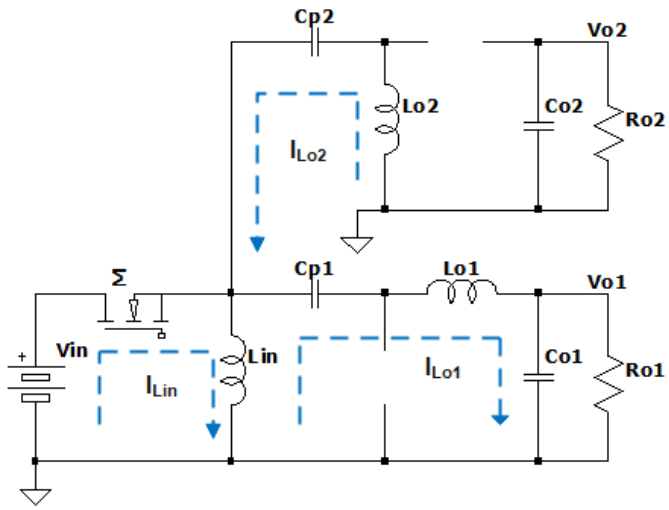


**Figure 4.** The proposed converter during $T_{on}$.

- During $T_{off}$ of M, both $D_{o1}$ and $D_{o2}$ are conducting. The inductors' currents' directions are shown in Figure 5.

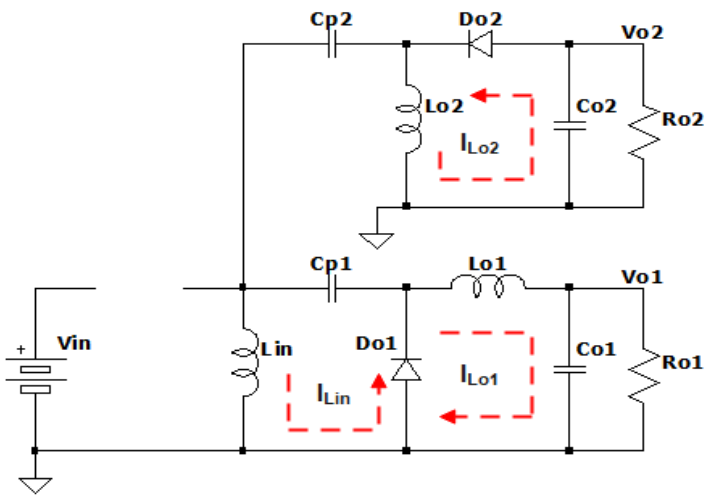


**Figure 5.** The proposed converter during $T_{off}$.

During this period, the inductors' currents are given by:

$$I_{Lin} = I_{Lin-max} - \frac{(V_{in} - V_{Cp1})}{L_{in}} t \tag{4}$$

$$I_{Lo1} = I_{Lo1-max} - \frac{V_{o1}}{L_{o1}} t \tag{5}$$

$$I_{Lo2} = I_{L2-max} - \frac{V_{o2}}{L_{o2}} t \tag{6}$$

where $T_{on} < t < T_s$, $T_s = T_{on} + T_{off}$. $I_{Lin-max}$, $I_{L1-max}$ and $I_{L2-max}$ are the upper limits of the inductor's currents.

- To calculate the duty cycle of the proposed converter, each converter has its own duty cycle, which is given by:

$$D_{zeta} = \frac{V_{o1}}{(V_{o1} + V_{in})} \tag{7}$$

and

$$D_{Mahafzah} = \frac{V_{o2}}{(V_{o2} + V_{in})} \tag{8}$$

The proposed converter has a duty cycle that can be calculated when connecting the common output voltage ($V_{o3}$) as follows:

$$V_{o3} = V_{o1} + V_{o2} \tag{9}$$

Substituting (7) and (8) in (9) yields:

$$V_{o3} = V_{in}\frac{D_M}{1 - D_M} + V_{in}\frac{D_M}{1 - D_M} \tag{10}$$

Solving for $D_M$ gives:

$$D_M = \frac{V_{o1} + V_{o2}}{2V_{in} + V_{o1} + V_{o2}} \tag{11}$$

And the voltage gain of the proposed converter is given by:

$$VG = \frac{V_{o3}}{V_{in}} = \frac{2D_M}{1 - D_M} \tag{12}$$

From (12) and Figure 6, it is clearly seen that the proposed converter has a boosting capability at lower duty cycles. Moreover, it has a higher voltage gain over the duty cycle range. Therefore, it is able to decrease the conduction losses of the selected switch.

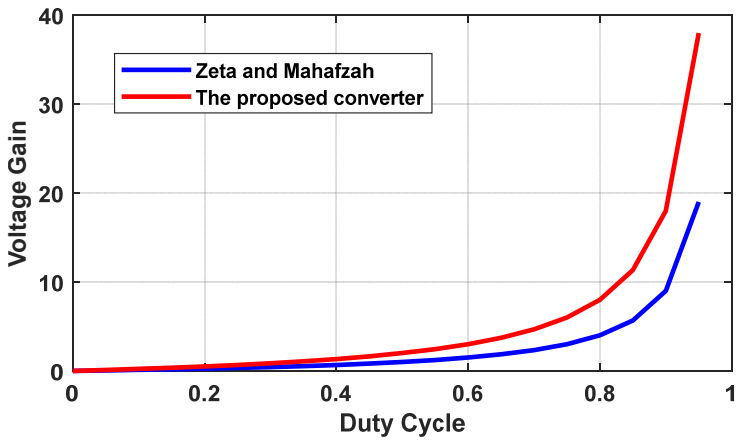


**Figure 6.** Voltage gain vs. duty cycle.

### *2.3. Design of the Proposed Hybrid Converter for AC–DC Adapter Applications*

As seen in Figure 3, the proposed hybrid converter includes one controlled switch, two diodes, three decoupled inductors, two coupling capacitors, and two low-pass filters (shunt filter capacitor with load resistance). The proposed hybrid converter is assumed to operate in continuous current mode (CCM) for the sake of simplicity. The discussion that follows demonstrates proper converter parameter selection for CCM operation mode. The components of the proposed hybrid converter are selected based on the procedure used in [31,32].

The design parameters are chosen to supply an electric vehicle; the DC output voltage (motor voltage) is 200 V (output voltage 3, see Figure 3). However, the load's rated output is 25 kW. Since the circuit will use an AC RMS line voltage as its input, the average rectified voltage is determined to be 200 V DC. The switching frequency is set at 20 kHz. All inductors' ripple current percentages are set to 20%. In contrast, the output voltage ripple should not be lower than 10% of the target output voltage. The selected design parameters and their associated values are shown in Table 2.

**Table 2.** Selected parameters of the design.

| The Selected Parameters | | The Calculated Parameters Based on [31,32] | |
|---|---|---|---|
| **Parameter** | **Value** | **Parameter** | **Value** |
| $P_{in}/P_o$ | 25 kW | $I_{o3}$ | 137 A |
| $V_{in\text{-}RMS}$ | 220 V | $I_{L1}$ | 240 A |
| $V_{o1}$ | 100 V | $I_{L2}$ | 240 A |
| $V_{o2}$ | −100 V | $I_{Lin}$ | 480 A |
| $V_{o3}$ | 200 V | $R_{o1}$ | 1 Ω |
| $\Delta I_{Lin}$ | 2 A | $R_{o2}$ | 1 Ω |
| $\Delta I_{L1}$ | 1 A | $R_{o3}$ | 1.5 Ω |
| $\Delta I_{L2}$ | 2 A | $I_{Lin}$ | 7.5 mH |
| $\Delta V_{Cp1}$ | <10 V | $L_1$ | 3 mH |
| $\Delta V_{Cp2}$ | <10 V | $L_2$ | 3 mH |
| *Duty Cycle (D)* | 50% | $C_{p1}$ | 200 µF |
| $f_s$ | 20 kHz | $C_{p2}$ | 200 µF |
| | | $C_{o1}$ | 1.2 mF |
| | | $C_{o2}$ | 1.2 mF |

Moreover, the proposed converter belongs to the category of DC–DC converters. As seen in Figure 3, it contains three inductors. The main milestone is the design (size) of these inductors. The inductor size is inversely proportional to the selected switching frequency. But increasing the switching frequency will deteriorate the converter efficiency. Therefore, selecting the switching frequency is a crucial issue.

### 2.4. Loss Calculations

To calculate the losses in Figure 3, Table 3 can be used. The losses in the proposed hybrid converter can be divided into three main types [36,37]: conduction loss, switching loss, and gate loss. In this paper, the passive devices are assumed to be ideal (no associated losses or the losses there are negligible). Then, the efficiency of the proposed hybrid converter is given by:

$$\eta = \frac{P_{out}}{P_{out} + P_{loss}} \tag{13}$$

where $P_{out}$ is the output power of the proposed hybrid converter, and $P_{loss}$ is the total power loss in the proposed hybrid converter, and it can be calculated using the equations in Table 3.

**Table 3.** Calculation of loss components [36,37].

| Losses Type | | Equation | Conditions |
|---|---|---|---|
| | | **Losses of Figure 3** | |
| Conduction Loss | In M | $P_{con-M} = \frac{R_{on-M}V_{in}^2}{3DR_s^2}$ | $R_{on}$: MOSFET m on-state resistance<br>$R_s$: Series resistance of the current loop |
| | In $D_{o1}$ or $D_{o2}$ | $P_{con-Df} = \frac{V_f V_{in}^2}{4V_o R_s}$ | $V_f$: Diode forward voltage |
| Switching Loss | In M | $P_{sw-M} = 0.5 f_s C_{oss}(0.5V_{in} + V_{o3})^2$ | $C_{oss}$: Switch M output capacitance |
| | In $D_{o1}$ or $D_{o2}$ | $P_{sw-M} = 0.5 f_s C_d(0.5V_{in} + V_{o3})^2$ | $C_d$: Diode parasitic capacitance |
| Control Loss | | $P_{g-M} = 2Q_M V_M f_s$ | $Q_g$: Switch gate charge<br>$V_g$: Voltage needed to charge the gate |
| Total Loss | | $P_t = P_{cond-M} + P_{cond-Do1} + P_{cond-Do2} + P_{sw-M} + P_{g-M}$ | |

## 3. Simulation Results

To assess the performance and efficacy of the proposed hybrid DC–DC converter, comprehensive simulations and experiments were conducted. The hybrid converter, composed

of a single controlled switch, multiple synchronized output voltages, two diodes, three inductors, and two coupling capacitors, was implemented in MATLAB/SIMULINK R2020a.

The simulations were carried out using parameters set at 25 kW, 200 V, and 130 A to represent real-world operating conditions. The simulation results demonstrated the significant improvement in voltage gain achieved by the novel hybrid converter as compared to conventional Zeta and Mahafzah topologies. The increased voltage gain was achieved at a lower duty cycle, effectively reducing the voltage stress across the output diodes and semiconductor switch. Consequently, the conduction losses were minimized, leading to higher overall efficiency and improved converter performance. The hybrid converter's operating concept and duty cycle calculations were thoroughly discussed, providing valuable insights into its behavior and control strategies.

To showcase the versatility and applicability of the proposed hybrid converter, it was evaluated in two distinct applications:

1. Application in Renewable Energy Systems: The hybrid converter was employed as a DC–DC converter in a renewable energy system. The results demonstrated its ability to efficiently convert and manage energy flows from renewable sources, making it a promising solution for sustainable energy applications.
2. Application as an Electric Vehicle Adapter (AC–DC Converter): The hybrid converter was tested as an AC–DC converter for electric vehicles. The simulation outcomes illustrated its capability to deliver reliable and regulated power supply to electric vehicles, highlighting its potential in the transportation sector.

Furthermore, the simulation results confirmed that the proposed hybrid converter can simultaneously support two separate loads with opposing energy flows, showcasing its adaptability and utility in complex power distribution scenarios.

In the context of the second application, the paper provided an analysis of the total harmonic distortion (THD) for the grid current. The results demonstrated that the new hybrid converter topology achieved a THD of 21.11% for the grid current. This indicates its effectiveness in mitigating harmonics and improving power quality in smart grid environments.

Overall, the simulation and experimental study validated the advantages and performance enhancements offered by the proposed hybrid DC–DC converter. Its ability to achieve higher voltage gain, reduce voltage stress, support multiple loads, and maintain synchronization between output voltages makes it a promising solution for smart grid applications, including renewable energy systems and electric vehicles. The outcomes of this study underscore the potential of the proposed hybrid converter to contribute to the advancement of power electronics and enhance the efficiency and reliability of modern power conversion technologies.

### *3.1. As a DC–DC Converter*

The proposed hybrid converter can be used in solar energy systems, as illustrated in Figure 7. The system comprises PV panels as a power supply, the proposed hybrid converter, and two power flow directions. As shown in Figure 7, the proposed converter can supply two different loads simultaneously. The positive energy flow (red arrow) represents the energy flow to the electrical grid through an inverter and/or transformer. In contrast to that, the other negative energy flow (green arrow) is used to recharge the energy storage system.

The two outputs of the proposed hybrid converter are illustrated in Figures 8 and 9. Figure 8 shows the negative voltage, which is responsible for recharging the energy storage system.

In contrast to that, Figure 9 depicts the output voltage, which is used to supply the inverter (red arrow in Figure 7).

The controlled switch M has a drain source voltage, as seen in Figure 10. As illustrated in Figure 10, the rated switch voltage is around 300 V. In addition to that, the switch current

is shown in Figure 11. The selected switch must be selected as IGBT because IGBT has high current capability. The average switch current is about 500 A.

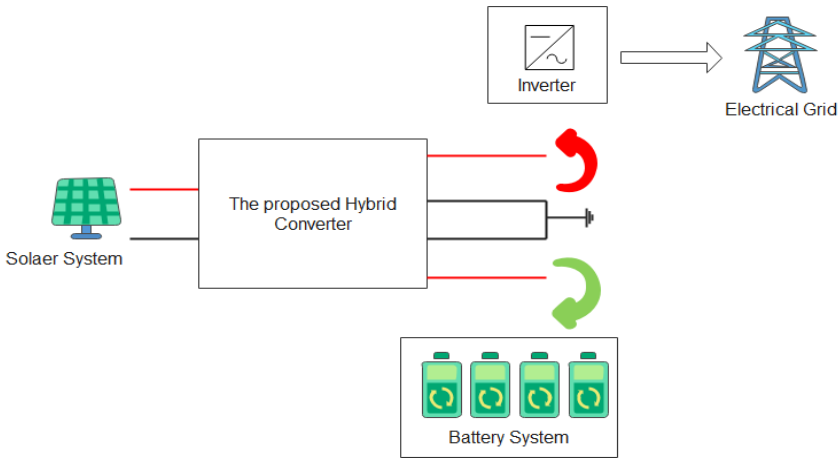


**Figure 7.** Connection of the proposed hybrid converter with a solar system.

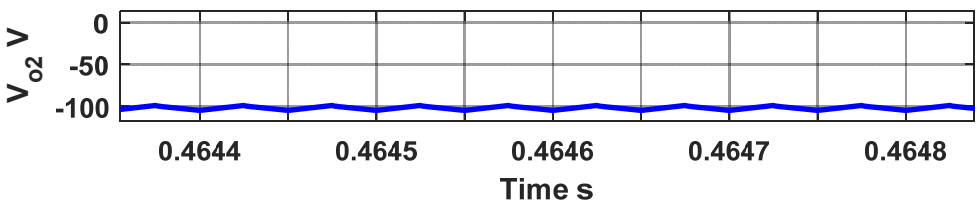


**Figure 8.** Negative voltage (green arrow in Figure 7).

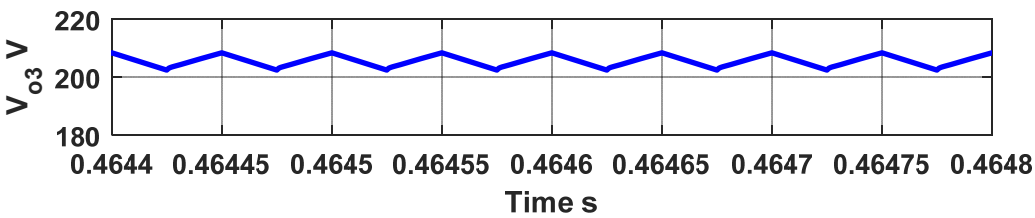


**Figure 9.** Positive output voltage (red arrow in Figure 7).

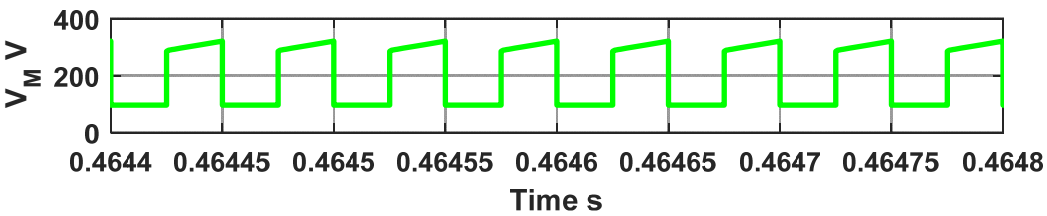


**Figure 10.** Switch M voltage.

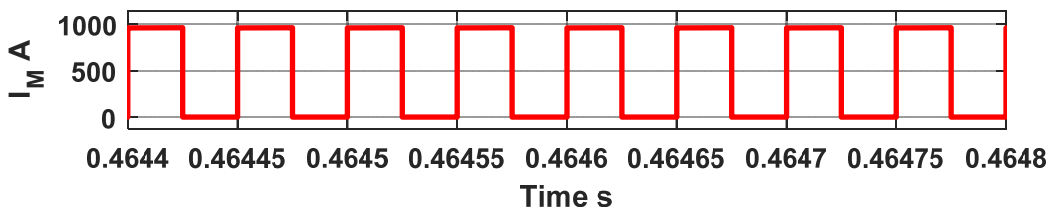


**Figure 11.** Switch M current.

Moreover, the diode $d_{o1}$ has voltage and current, as shown in Figures 12 and 13, respectively. The diode must be selected as a silicon diode, which can carry about 250 A.

On the other hand, the diode do2 voltage and current are shown in Figures 14 and 15, respectively. Again, the diode 2 average current is about 250 A. From Figure 15, the diode 2 pulsating current is about 1000 A. This value can be reduced when applying a soft switching topology.

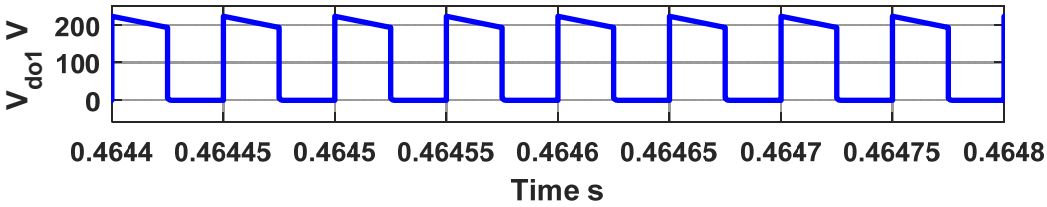


**Figure 12.** Diode $d_{o1}$ voltage.

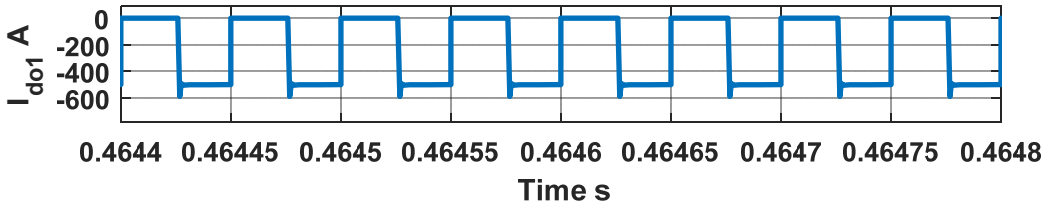


**Figure 13.** Diode $d_{o1}$ current.

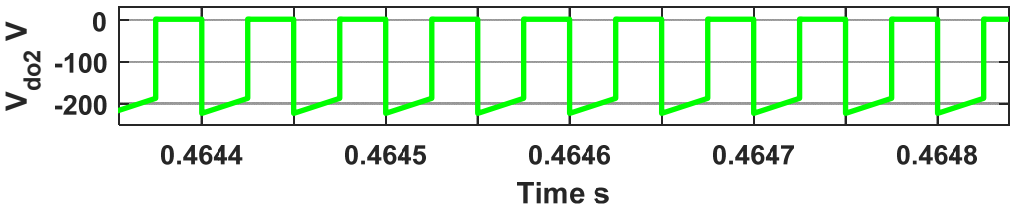


**Figure 14.** Diode $d_{o2}$ voltage.

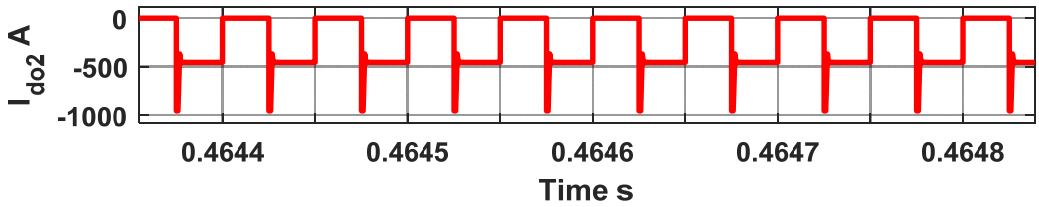


**Figure 15.** Diode $d_{o2}$ current.

The simulation in this paper is applied, and the parameters are used to ensure that the proposed hybrid converter operates in continuous conduction mode (CCM). This mode of operation can be clearly seen in the inductors' ($L_{in}$, $L_{o1}$, and $L_{o2}$) currents, which are illustrated in Figures 16–18, respectively. The main inductor, $L_{in}$, has a current equal to the sum of the $L_{o1}$ and $L_{o2}$ currents. The inductors' currents have a low current ripple, as discussed before. In addition to that, the inductors' voltages are shown in Figures 19–21. The average inductor voltages are zero, which ensures the stability of the proposed hybrid converter.

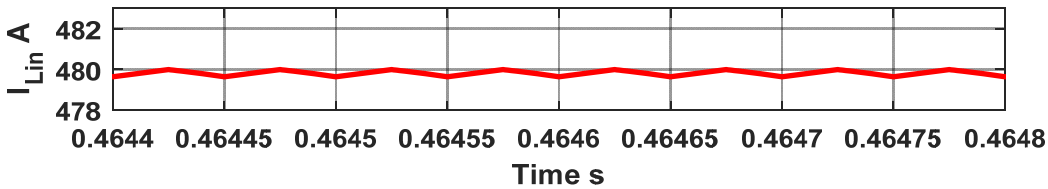


**Figure 16.** Inductor $L_{in}$ current.

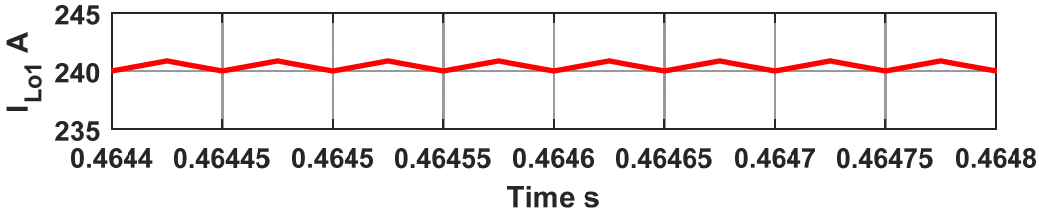


**Figure 17.** Inductor $L_{o1}$ current.

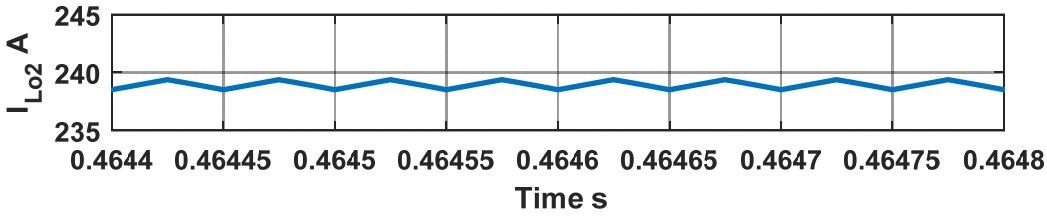


**Figure 18.** Inductor $L_{o2}$ current.

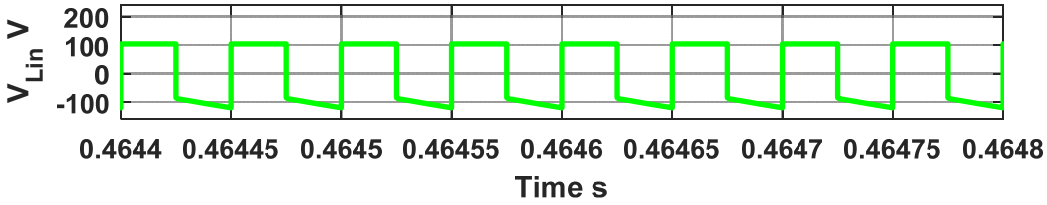


**Figure 19.** Inductor $L_{in}$ voltage.

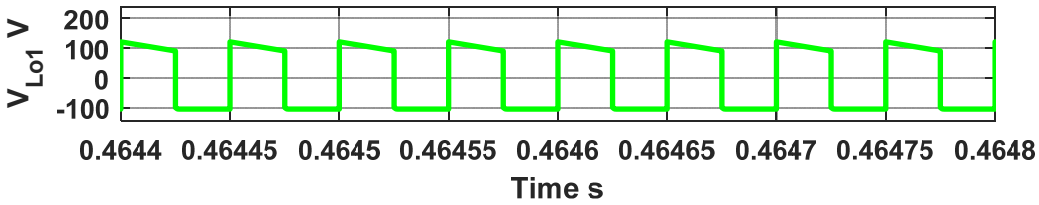


**Figure 20.** Inductor $L_{o1}$ voltage.

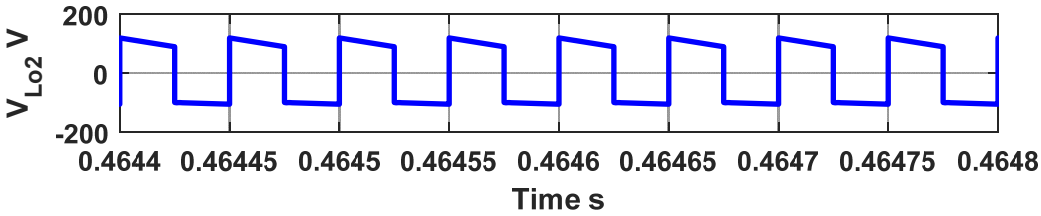


**Figure 21.** Inductor $L_{o2}$ voltage.

### *3.2. As an AC–DC Converter*

Electric vehicles require an AC–DC converter to recharge their auxiliary systems. This comprises two stages: First, the AC–DC converter (diode bridge rectifier) is cascaded with the DC–DC converter. The proposed hybrid converter is employed to regulate the output voltage. To simulate the AC–DC converter, a full-bridge diode rectifier is connected to the grid to achieve a positive rectified voltage. After that, the rectified voltage is chopped by the proposed hybrid converter to achieve the desired output voltages. This application is shown in Figure 22.

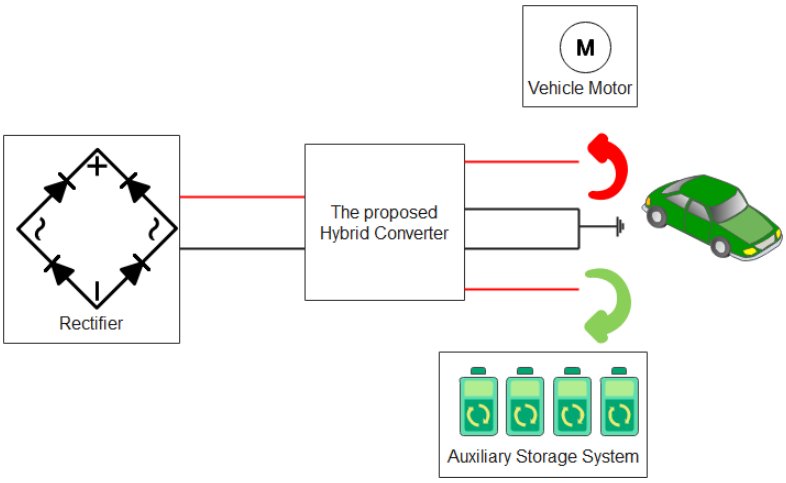


**Figure 22.** The proposed hybrid converter in EV adapter applications.

As shown in Figure 23a, the output voltage Vo1 is regulated around 100 V. The other output voltage, $V_{o2}$, is regulated to −100 V, see Figure 23b. Finally, the output voltage, $V_{o3}$, is set to 200 V, see Figure 23c. Since the load is DC load and its value is 1.5 Ω, the load current is in phase with the load voltage. It provides an approximately 130 A load voltage, see Figure 24.

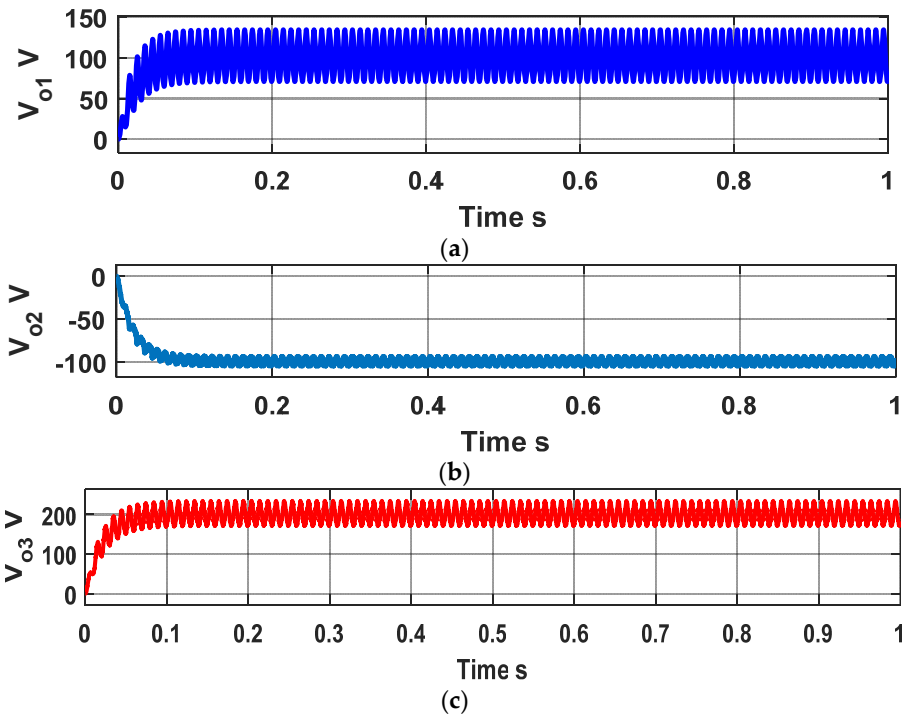


**Figure 23.** The output voltages of the proposed hybrid converter. (**a**) the load 1 output voltage. (**b**) the load 2 output voltage. (**c**) the load 3 output voltage.

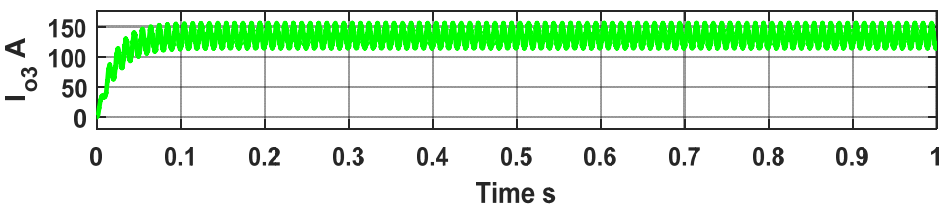


**Figure 24.** The load current.

The rectified voltage of the grid voltage is seen in Figure 25a. This rectified voltage is regulated by the proposed hybrid converter. The grid current is affected by the switching behavior of the grid current. This could disturb the grid current, see the average grid current in Figure 25b. To estimate the power factor (PF) of the grid current, the following equation could be used:

$$PF = Distortion\ Factor \times Displacement\ Factor \tag{14}$$

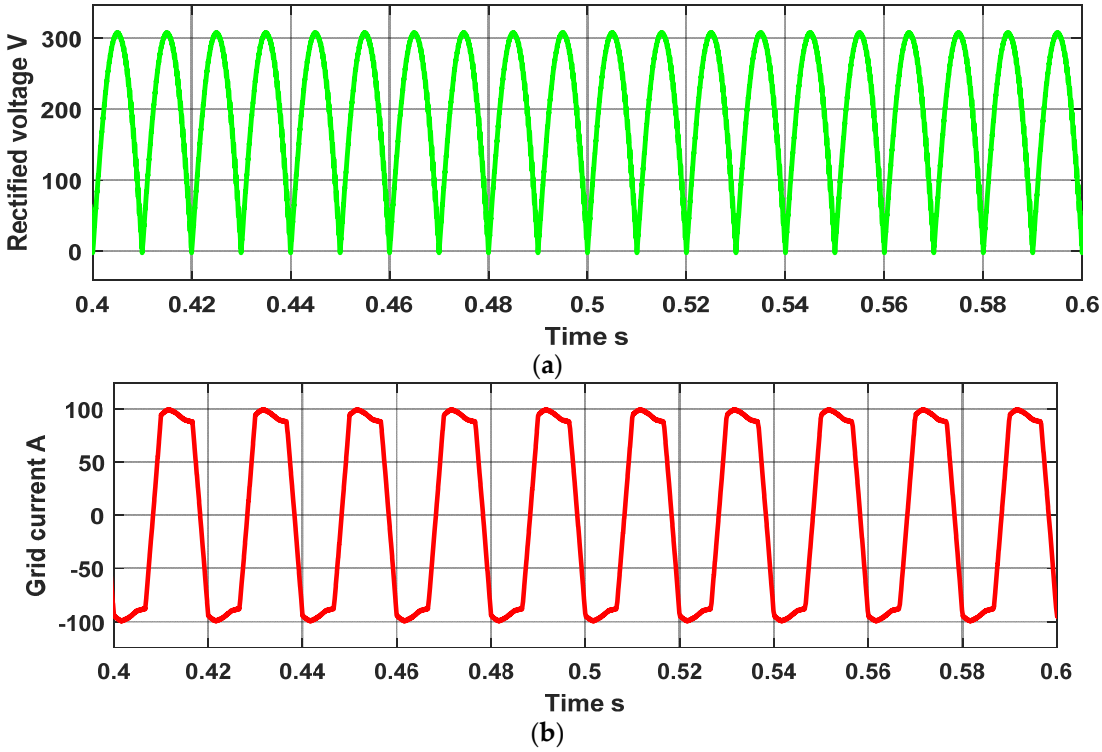


**Figure 25.** Rectified grid voltage and grid current. (**a**) Rectified voltage. (**b**) Grid current.

In this case, the load is a DC load; therefore, the displacement factor is 1 (cos θ = 1). Thus, the distortion factor is estimated in this case only by calculating:

$$Distortion\ Factor\ (DF) = \frac{I_{in,1,rms}}{I_{in,t,rms}} \tag{15}$$

where $I_{in,1,rms}$ is the fundamental RMS grid current, and $I_{in,t,rms}$ is the total RMS grid current. Finally, the total harmonic distortion (*THD*) is calculated by:

$$THD = \sqrt{\frac{1}{DF^2} - 1} \tag{16}$$

The *THD* of the grid current is illustrated in Figure 26. It can be seen that the *THD* of the grid current is about 21.11%. This value is within the IEEE 519 standards [38], but in future works, it could be possible to further reduce this value because the main contributor is the third harmonic. To reduce this value, a proper filter design could be the solution. However, the proposed hybrid converter has a low distortion effect on the electrical grid.

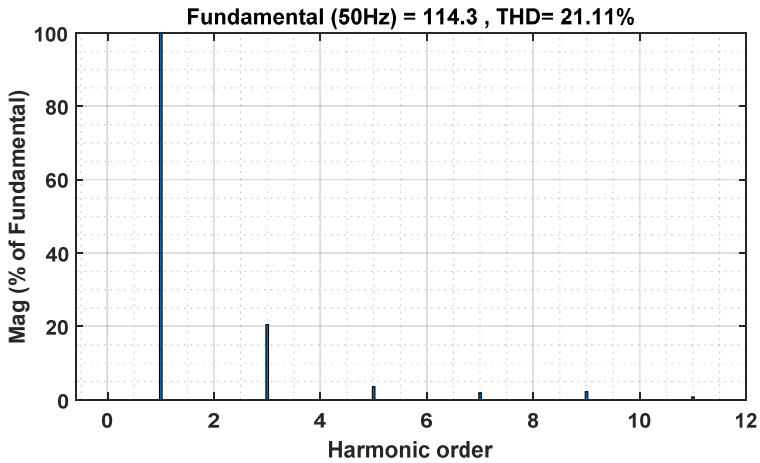


**Figure 26.** THD of the grid current.

### 3.3. Cost Analysis

Figures 1–3 show the main converters in the paper. The next table summarizes the main components of each converter. As seen in Table 4, the proposed converter has only one switch compared with the other two converters. However, the proposed converter has a higher number of components (diodes, inductors, coupling capacitors, and low-pass filters). Therefore, it has a higher cost compared with other individual converters. The cost of components differs based on the selected components (electrical and thermal characteristics), the power range, the manufacturer, and the supplier. Check [39,40].

**Table 4.** Component comparison.

| Component | Zeta Converter | Mahafzah Converter | Proposed Converter |
|---|---|---|---|
| Number of switches | 1 | 1 | 1 |
| Number of diodes | 1 | 1 | 2 |
| Number of capacitors | 1 | 1 | 2 |
| Number of inductors | 2 | 2 | 3 |
| Output low pass filter | 1 | 1 | 2 |

The proposed converter distinguishes itself from conventional designs, such as the Zeta and Mahafzah converters, by incorporating a higher count of passive components.

These additional passive components play a crucial role in facilitating the smooth transfer of energy to the load side. Unlike its counterparts, the proposed converter employs this surplus of passive elements specifically to enhance the efficiency and effectiveness of energy transmission. It's noteworthy that, despite the increased number of passive components, the proposed converter maintains parity with the Zeta and Mahafzah converters in terms of the passive components involved in energy transfer during each mode of operation. This ensures that, while the converter benefits from enhanced functionality, it does not sacrifice the fundamental principles of energy conversion efficiency.

## 4. Conclusions

In this paper, a new hybrid DC–DC converter based on Mahafzah and Zeta converters was proposed. The proposed hybrid converter is made up of a single controlled switch, several synchronized output voltages, two diodes, three inductors, and two coupling capacitors. In comparison to the Zeta and Mahafzah topologies, the novel converter is able to double the voltage gain, yielding a higher voltage gain at a lower duty cycle. This benefit can decrease the voltage stress across the output diodes and semiconductor switches. The paper presents an extensive discussion about the hybrid converter's operating concept. Additionally, the duty cycle was determined. The proposed hybrid converter's employment in two distinct applications was presented in the study. The new converter's first application

was as a DC–DC converter in a system for renewable energy. The second was using the new converter as an adaptor (AC–DC converter) for electric vehicles. A simulation at 25 kW, 200 V, and 130 A was performed using MATLAB/SIMULINK to demonstrate the efficacy of the suggested hybrid converter. The outcomes demonstrated the new converter's capacity to support two separate loads with opposing energy flows. In the case of the second application, the analysis of the total harmonic distortion (THD) for the grid current was also provided. When using the new hybrid converter topology, a 21.11% THD of the grid current is attained.

**Author Contributions:** Conceptualization, K.A.M. methodology, K.A.M. and M.A.O.; software, K.A.M.; validation, K.A.M., M.A.O., A.M., E.R.S. and G.Z.; formal analysis, K.A.M.; investigation, K.A.M. and M.A.O.; writing—original draft preparation, K.A.M., M.A.O. and A.M.; writing—review and editing, E.R.S. and G.Z.; visualization, K.A.M., M.A.O., A.M. and E.R.S.; supervision, E.R.S. All authors have read and agreed to the published version of the manuscript.

**Funding:** This research received no external funding.

**Data Availability Statement:** Data available on request due to restrictions. The data presented in this study on request from the corresponding author due to the privacy reasons.

**Conflicts of Interest:** The authors declare no conflicts of interest.

## References

1. Gaboriault, M.; Notman, A. A high efficiency, noninverting, buck-boost DC-DC converter. In Proceedings of the Nineteenth Annual IEEE Applied Power Electronics Conference and Exposition, 2004, APEC'04, Anaheim, CA, USA, 22–26 February 2004; IEEE: Piscataway, NJ, USA, 2004; Volume 3.
2. Banaei, M.R.; Bonab, H.A.F. A high efficiency nonisolated buck–boost converter based on ZETA converter. *IEEE Trans. Ind. Electron.* **2019**, *67*, 1991–1998. [CrossRef]
3. Li, W.; Fan, L.; Zhao, Y.; He, X.; Xu, D.; Wu, B. High-step-up and high-efficiency fuel-cell power-generation system with active-clamp flyback–forward converter. *IEEE Trans. Ind. Electron.* **2011**, *59*, 599–610.
4. Vu, H.-N.; Choi, W. A novel dual full-bridge LLC resonant converter for CC and CV charges of batteries for electric vehicles. *IEEE Trans. Ind. Electron.* **2017**, *65*, 2212–2225. [CrossRef]
5. Mahafzah, K.A.; Obeidat, M.A.; Al-Shetwi, A.Q.; Ustun, T.S. A Novel Synchronized Multiple Output DC-DC Converter Based on Hybrid Flyback-Cuk Topologies. *Batteries* **2022**, *8*, 93. [CrossRef]
6. Mahafzah, K.A.; Rababah, H.A. A novel step-up/step-down DC-DC converter based on flyback and SEPIC topologies with improved voltage gain. *Int. J. Power Electron. Drive Syst. (IJPEDS)* **2023**, *14*, 898–908. [CrossRef]
7. Hwu, K.I.; Peng, T.J. A novel buck–boost converter combining KY and buck converters. *IEEE Trans. Power Electron.* **2011**, *27*, 2236–2241. [CrossRef]
8. Zhang, Y.; Paresh, C.S. A new soft-switching technique for buck, boost, and buck-boost converters. *IEEE Trans. Ind. Appl.* **2003**, *39*, 1775–1782. [CrossRef]
9. Lefeuvre, E.; Audigier, D.; Richard, C.; Guyomar, D. Buck-boost converter for sensorless power optimization of piezoelectric energy harvester. *IEEE Trans. Power Electron.* **2007**, *22*, 2018–2025. [CrossRef]
10. Cordeiro, A.; Chaves, M.; Canacsinh, H.; Luis, R.; Pires, V.F.; Foito, D.; Pires, A.J.; Martins, J.F. Hybrid Sepic-Cuk DC-DC Converter Associated to a SRM Drive for a Solar PV Powered Water Pumping System. In Proceedings of the 2019 8th International Conference on Renewable Energy Research and Applications (ICRERA), Brasov, Romania, 3–6 November 2019; pp. 169–174. [CrossRef]
11. Chakraborty, S.; Reza, S.M.S.; Hasan, W. Design and analysis of hybrid solar-wind energy system using CUK & SEPIC converters for grid connected inverter application. In Proceedings of the 2015 IEEE 11th International Conference on Power Electronics and Drive Systems, Sydney, NSW, Australia, 9–12 June 2015; pp. 278–283. [CrossRef]
12. Haque, M.Z.; Al Hysam, M.A.; Rahman, A.; Ihsan, M.A.; Ahmed, S.; Molla, N.M. A Hybrid Bipolar DC-Link Converter Based on SEPIC-Cuk Combination. In Proceedings of the 2022 4th International Conference on Sustainable Technologies for Industry 4.0 (STI), Dhaka, Bangladesh, 17–18 December 2022; pp. 1–5. [CrossRef]
13. Suresh, K.V.; Vinayaka, K.U.; Rajesh, U. A CUK-SEPIC fused converter topology for wind-solar hybrid systems for stand-alone systems. In Proceedings of the 2015 IEEE Power, Communication and Information Technology Conference (PCITC), Bhubaneswar, India, 15–17 October 2015; pp. 48–53. [CrossRef]
14. Lodh, T.; Majumder, T. High gain and efficient integrated flyback-Sepic DC-DC converter with leakage energy recovery mechanism. In Proceedings of the 2016 International Conference on Signal Processing, Communication, Power and Embedded System (SCOPES), Paralakhemundi, India, 3–5 October 2016; pp. 1495–1500. [CrossRef]
15. Saket, M.A.; Ordonez, M.; Shafiei, N. Planar transformers with near-zero common-mode noise for flyback and forward converters. *IEEE Trans. Power Electron.* **2017**, *33*, 1554–1571. [CrossRef]

16. Wang, D.; He, X.; Shi, J. Design and analysis of an interleaved flyback–forward boost converter with the current autobalance characteristic. *IEEE Trans. Power Electron.* **2009**, *25*, 489–498. [CrossRef]
17. Eshkevari, A.L.; Mosallanejad, A.; Sepasian, M. Design, modelling, and implementation of a modified double-switch flyback-forward converter for low power applications. *IET Power Electron.* **2019**, *12*, 739–748. [CrossRef]
18. Xie, X.; Li, J.; Peng, K.; Zhao, C.; Lu, Q. Study on the single-stage forward-flyback PFC converter with QR control. *IEEE Trans. Power Electron.* **2015**, *31*, 430–442. [CrossRef]
19. Kundu, U.; Yenduri, K.; Sensarma, P. Accurate ZVS analysis for magnetic design and efficiency improvement of full-bridge LLC resonant converter. *IEEE Trans. Power Electron.* **2016**, *32*, 1703–1706. [CrossRef]
20. Wu, S.-T.; Han, C.-H. Design and implementation of a full-bridge LLC converter with wireless power transfer for dual mode output load. *IEEE Access* **2021**, *9*, 120392–120406. [CrossRef]
21. Shen, Y.; Zhao, W.; Chen, Z.; Cai, C. Full-bridge LLC resonant converter with series-parallel connected transformers for electric vehicle on-board charger. *IEEE Access* **2018**, *6*, 13490–13500. [CrossRef]
22. Salem, M.; Ramachandaramurthy, V.K.; Sanjeevikumar, P.; Leonowicz, Z.; Yaramasu, V. Full bridge LLC resonant three-phase interleaved multi converter for HV applications. In Proceedings of the 2019 IEEE International Conference on Environment and Electrical Engineering and 2019 IEEE Industrial and Commercial Power Systems Europe (EEEIC/I&CPS Europe), Genova, Italy, 11–14 June 2019; IEEE: Piscataway, NJ, USA, 2019.
23. Bakas, P.; Okazaki, Y.; Shukla, A.; Patro, S.K.; Ilves, K.; Dijkhuizen, F.; Nami, A. Review of hybrid multilevel converter topologies utilizing thyristors for HVDC applications. *IEEE Trans. Power Electron.* **2020**, *36*, 174–190. [CrossRef]
24. Zhang, J.; Xu, S.; Din, Z.; Hu, X. Hybrid multilevel converters: Topologies, evolutions and verifications. *Energies* **2019**, *12*, 615. [CrossRef]
25. Li, Y.; Zhao, Y. A virtual space vector model predictive control for a seven-level hybrid multilevel converter. *IEEE Trans. Power Electron.* **2020**, *36*, 3396–3407. [CrossRef]
26. Mathew, E.C.; Ghat, M.B.; Shukla, A. A generalized cross-connected submodule structure for hybrid multilevel converters. *IEEE Trans. Ind. Appl.* **2016**, *52*, 3159–3170. [CrossRef]
27. Li, Y.; Diao, F.; Zhao, Y. Simplified two-stage model predictive control for a hybrid multilevel converter with floating H-bridge. *IEEE Trans. Power Electron.* **2020**, *36*, 4839–4850. [CrossRef]
28. Lodh, T.; Majumder, T. A high gain high-efficiency negative output flyback-Cuk integrated DC-DC converter. In Proceedings of the 2016 International Conference on Signal Processing, Communication, Power and Embedded System (SCOPES), Paralakhemundi, India, 3–5 October 2016; IEEE: Piscataway, NJ, USA, 2016.
29. Buso, S.; Spiazzi, G.; Tagliavia, D. Simplified control technique for high-power-factor flyback Cuk and Sepic rectifiers operating in CCM. *IEEE Trans. Ind. Appl.* **2000**, *36*, 1413–1418. [CrossRef]
30. Ji, Y.H.; Kim, J.H.; Jang, S.J.; Won, C.Y.; Kim, S.S. Fuel cell generation system with SEPIC-flyback converter. In Proceedings of the 2nd International Conference on Ubiquitous Information Management and Communication, Suwon, Republic of Korea, 31 January–1 February 2008.
31. Reddy, P.L.S.K.; Obulesu, Y.P.; Singirikonda, S.; Al Harthi, M.; Alzaidi, M.S.; Ghoneim, S.S.M. A Non-Isolated Hybrid Zeta Converter with a High Voltage Gain and Reduced Size of Components. *Electronics* **2022**, *11*, 483. [CrossRef]
32. Mahafzah, K.A.; Al-Shetwi, A.Q.; Hannan, M.A.; Babu, T.S.; Nwulu, N. A New Cuk-Based DC-DC Converter with Improved Efficiency and Lower Rated Voltage of Coupling Capacitor. *Sustainability* **2023**, *15*, 8515. [CrossRef]
33. Wu, P.; Huang, W.; Tai, N.; Liang, S. A novel design of architecture and control for multiple microgrids with hybrid AC/DC connection. *Appl. Energy* **2018**, *210*, 1002–1016. [CrossRef]
34. Charadi, S.; Chaibi, Y.; Redouane, A.; Allouhi, A.; El Hasnaoui, A.; Mahmoudi, H. Efficiency and energy-loss analysis for hybrid AC/DC distribution systems and microgrids: A review. *Int. Trans. Electr. Energy Syst.* **2021**, *31*, e13203. [CrossRef]
35. Saponara, S.; Saletti, R.; Mihet-Popa, L. Recent Trends in DC and Hybrid Microgrids: Opportunities from Renewables Sources, Battery Energy Storages and Bi-Directional Converters. *Appl. Sci.* **2020**, *10*, 4388. [CrossRef]
36. Mahafzah, K.A.; Krischan, K.; Muetze, A. Efficiency enhancement of a three phase Hard Switching Inverter under light load conditions. In Proceedings of the IECON 2016-42nd Annual Conference of the IEEE Industrial Electronics Society, Florence, Italy, 23–26 October 2016; IEEE: Piscataway, NJ, USA, 2016; pp. 3372–3377.
37. Mahafzah, K.A.; Krischan, K.; Muetze, A. Efficiency enhancement of a three phase Soft Switching Inverter under light load conditions. In Proceedings of the IECON 2016-42nd Annual Conference of the IEEE Industrial Electronics Society, Florence, Italy, 23–26 October 2016; IEEE: Piscataway, NJ, USA, 2016; pp. 3378–3383.
38. Available online: https://www.elspec-ltd.com/ieee-519-2014-standard-for-harmonics/ (accessed on 29 February 2024).
39. Available online: https://uk.rs-online.com/web/ (accessed on 28 February 2024).
40. Available online: https://export.farnell.com/ (accessed on 29 February 2024).


**Disclaimer/Publisher's Note:** The statements, opinions and data contained in all publications are solely those of the individual author(s) and contributor(s) and not of MDPI and/or the editor(s). MDPI and/or the editor(s) disclaim responsibility for any injury to people or property resulting from any ideas, methods, instructions or products referred to in the content.